J Therm Anal Calorim (2009) 97:245–250
DOI 10.1007/s10973-009-0250-x

Preparation of $Co_xFe_{3-x}O_4$ nanoparticles by thermal decomposition of some organo-metallic precursors

**Mircea Stefanescu · Marcela Stoia ·
Costica Caizer · Thomas Dippong · Paul Barvinschi**

ICTAC2008 Conference

Abstract This paper presents a study for the preparation of $Co_xFe_{3-x}O_4$ ($x = 0.02$, 0.2, 0.5, 0.8, 1.0, 1.1, 1.5) nanoparticles, starting from metal nitrates: $Co(NO_3)_2 \cdot 6H_2O$, $Fe(NO_3)_3 \cdot 9H_2O$ and ethylene glycol ($C_2H_6O_2$). By heating the solutions metal nitrates-ethylene glycol, the redox reaction took place between the anion NO_3^- and $OH–(CH_2)_2–OH$ with formation of carboxylate anions. The resulted carboxylate anions reacted with Co(II) and Fe(III) cations to form coordinative compounds which are precursors for cobalt ferrite. XRD and magnetic measurements have evidenced the formation of cobalt ferrite for all studied molar ratios. The average diameter of the cobalt ferrite crystallites was estimated from XRD data and showed values in the range 10–20 nm. The crystallites size depends on the annealing temperature. The magnetization of the synthesized samples depends on the molar ratio Co/Fe and on the annealing temperature.

Keywords Carboxylate · Cobalt ferrite · Thermal analysis

Introduction

Inorganic mixed oxides attract much attention due to their properties that recommend them for multiple practical applications [1, 2]. Between them, cobalt ferrite as nanoparticles is an interesting material due to its magneto-crystalline anisotropy, high coercivity, moderate saturation magnetization, high chemical stability, wear resistance and electric insulation [3]. These properties indicate a high physical and chemical stability. $CoFe_2O_4$ presents applications in micro production industry, high performance digital tapes, refrigerators, ferrofluids and intensifying of magnetic resonance [4].

Cobalt ferrite crystallizes in a partially inverse spinel structure with the formula $(Co_\delta Fe_{1-\delta})[Co_{1-\delta}Fe_{1+\delta}]O_4$, where by () and [] were indicated the tetrahedral and octahedral sites and δ depends on thermal history. Since the $Fe_A^{3+} - Fe_B^{3+}$ super exchange interaction differs from the $Co_A^{2+} - Fe_B^{3+}$ interaction, variation of the cation distribution over the A and B sites in the spinel leads to different magnetic properties of the ferrite even for the same composition [5]. The methods reported in the literature for preparation of cobalt ferrite nanoparticles with variable composition ($Co_xFe_{3-x}O_4$) are: method of micro-emulsions [6], co-precipitation [2], hydrothermal method [7], thermal decomposition of some precursors [8] and combustion reaction method [3]. Few studies have been reported in the literature on the system ($Co_xFe_{3-x}O_4$) as nanoparticles for large x (0.05–1.5) value ranges. These studies have followed the magnetic properties of the system in order to understand the high anisotropy of Co atoms in the spinel structure [9].

In this paper, we present a study on the preparation of the oxidic system $Co_xFe_{3-x}O_4$ for $x = 0.02$, 0.2, 0.5, 0.8, 1.0, 1.1 and 1.5 starting from a mixture of Fe(III), Co(II) nitrates and ethylene glycol (EG). During the heating of this mixture, a redox reaction takes place between the nitrate ion and ethylene glycol with formation of Co(II) and Fe(III) carboxylates, further used as precursors of

M. Stefanescu (✉) · M. Stoia · T. Dippong
Faculty of Industrial Chemistry and Environmental Engineering,
University "Politehnica" of Timisoara, P-ta Victoriei nr. 2,
300006 Timisoara, Romania
e-mail: mircea.stefanescu@chim.upt.ro

C. Caizer · P. Barvinschi
Faculty of Physics, West University of Timisoara,
Bv. V. Parvan No. 4, 300223 Timisoara, Romania

$Co_xFe_{3-x}O_4$ oxides. We have studied the evolution of the crystalline phases with the annealing temperature, depending on the Co/Fe ratio introduced in synthesis. The magnetic properties of the annealing products at 400, 700 and 1,000 °C have been correlated with their composition and the particles dimensions.

Experimental

The synthesis of Co(II) and Fe(III) carboxylates, precursors of the system $Co_xFe_{3-x}O_4$, was achieved by the redox reaction between the metal nitrates and ethylene glycol. The progress of the redox reaction was studied by DTA on a 1500 MOM Budapesta derivatograph. The solution $Fe(NO_3)_3$–$Co(NO_3)_2$–$C_2H_6O_2$ was disposed in thin layer on Pt plates.

The precursors of cobalt ferrite were synthesized at 130 °C for different molar ratios $Fe(NO_3)_3$:$Co(NO_3)_2$, corresponding to the preparation of the $Co_xFe_{3-x}O_4$ system for ($x = 0.02$, 0.2, 0.5, 0.8, 1.0, 1.1 and 1.5) according to Table 1.

All synthesized precursors were analysed by FT-IR spectrometry using a FT-IR Prestige-21, Shimadzu spectrometer and by thermal analysis with a Mettler TGA/FDTA/851LF/1100.

We have decomposed the precursors (P_1–P_7) at 300 °C, 3 h and than annealed them at 400, 700 and 1,000 °C, for 3 h. The annealing products were characterized by XRD with a diffractometer D8 Advanced-Bruker AXS, using Mo-K_α ($\lambda_{Mo} = 0.7093$ Å) radiation and by FT-IR. The magnetic measurements have been performed on a laboratory installation with data acquisition system.

Results and discussions

Our previous studies on the redox reaction $Fe(NO_3)_3$-diol [11] and $Co(NO_3)_2$-diol [10, 12], have evidenced that this reaction takes place at ~70 °C for $Fe(NO_3)_3$-diol and at ~120 °C for $Co(NO_3)_2$-diol with formation of Fe(III) and Co(II) carboxylates type complexes.

In this paper, in order to obtain precursors of the system $Co_xFe_{3-x}O_4$, we have started from the mixture of two metal nitrates ($Fe(NO_3)_3\cdot 9H_2O$ and $Co(NO_3)_2\cdot 6H_2O$), in different molar ratios, and ethylene glycol. The thermal behaviour of the solutions $Fe(NO_3)_3$–$Co(NO_3)_2$–EG solutions was studied by DTA.

Figure 1 presents the thermal curves for the mixture corresponding to the samples P_3, P_5 and P_7, molar ratio $Fe(NO_3)_3$:$Co(NO_3)_2$ of 5 ($x = 0.5$), 2 ($x = 1$) and 1 ($x = 1.5$).

The exothermic effect registered at low temperature (70 °C) can be attributed to the redox reaction $Fe(NO_3)_3$–EG, due to the stronger acidity of the aqua-cation $[Fe(H_2O)_6]^{3+}$. The effect from 120 °C, which appears on DTA curves of the samples P_3 (1), P_5 (2) and P_7 (3) with a higher Co content, can be assigned to the redox reaction $Co(NO_3)_2$–EG. The result of these redox reactions is most probable the formation of a homogenous mixture of homonuclear Fe(III) and Co(II) carboxylates. The exothermic effect from 300 °C is attributed to the oxidative decomposition of the metal carboxylates mixture.

All other synthesized samples exhibit similar thermal behaviour, with exothermic effects which depend on the ratio $Fe(NO_3)_3$/$Co(NO_3)_2$. Based on thermal analysis we have established 130 °C as optimal synthesis temperature for the oxides precursors. The obtained precursors were characterized using FT-IR and thermal analysis. FT-IR analysis has evidenced the formation of metal carboxylates in all synthesized precursors.

Figure 2 presents the FT-IR spectra for the precursors P_3, P_5 and P_7, obtained at 130 °C for different Fe:Co ratios (see Table 1).

The presence of the carboxylate group coordinated by the metal ions was evidenced by the characteristic bands: at ~1,620 cm^{-1} the band attributed to the vibration ν_{as} (COO^-) and in the range 1,300–1,400 cm^{-1} the bands attributed to the vibrations $\nu_s(COO^-)$ (~1,360 cm^{-1}) and $\nu_s(CO) + \delta(OCO)$ (~1,320 cm^{-1}) [13].

Table 1 Characteristics of the synthesized samples

Sample	Molar ratio $Fe(NO_3)_3$:$Co(NO_3)_2$	Molar ratio NO_3^-:EG	Value for x corresponding to $Co_xFe_{3-x}O_4$
P_1	149:1	1:1	0.02
P_2	14:1	1:1	0.2
P_3	5:1	1:1	0.5
P_4	2.75:1	1:1	0.8
P_5	2:1	1:1	1.0
P_6	1.7:1	1:1	1.1
P_7	1:1	1:1	1.5

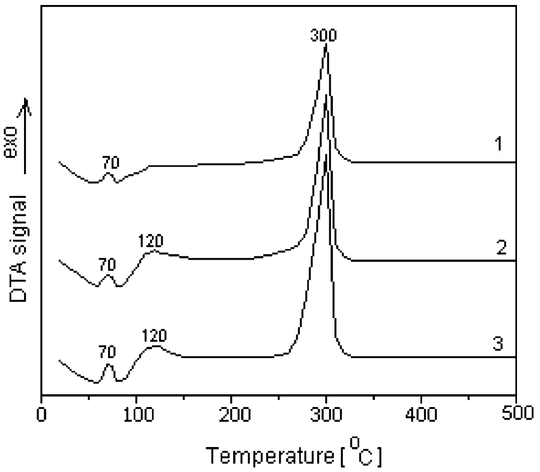

Fig. 1 DTA of the solutions $Co(NO_3)_2$–$Fe(NO_3)_3$–EG corresponding to samples: P_3 (1), P_5 (2), P_7 (3)

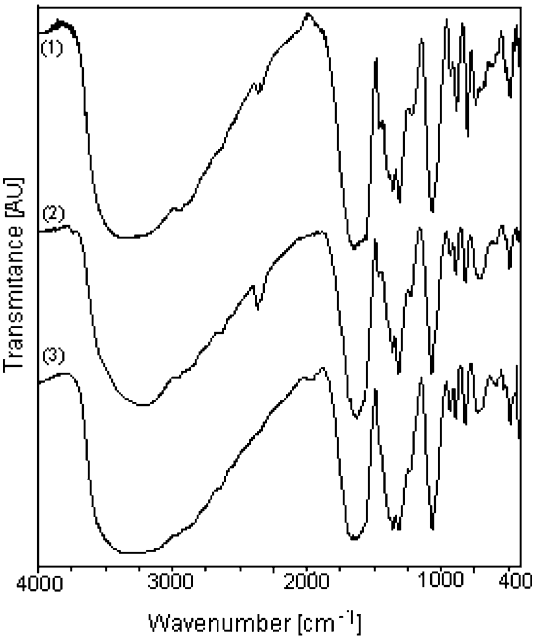

Fig. 2 FT-IR spectra of the precursors synthesized at 130 °C: P_3 (1), P_5 (2) and P_7 (3)

The thermal behaviour of the synthesized precursors was studied by thermal analysis (TG and DTA). Figure 3a–c presents the derivatograms recorded at air heating up to 500 °C, of the precursors P_3, P_5 and P_7 for molar ratios Fe(III):Co(II) of 5 (x = 0.5), 2 (x = 1) and 1 (x = 0.5).

The evolutions of the registered thermal curves show a similar thermal behaviour for the investigated samples. The first two endothermic stages of decomposition, up to 200 °C, correspond to the loss of associated and coordinated water molecules. The oxidative decomposition of the

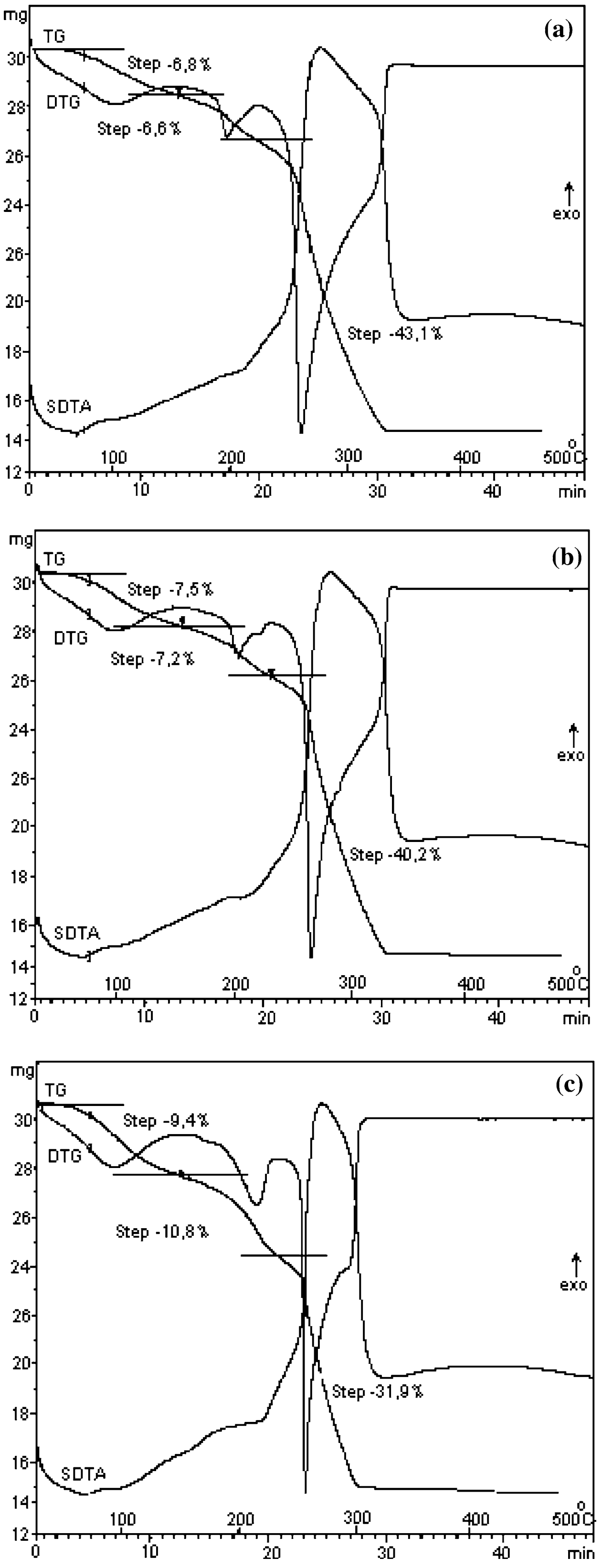

Fig. 3 TG and DTA of the precursors synthesized at 130 °C: P_3 (**a**), P_5 (**b**) and P_7 (**c**)

precursors takes place in the range 230–330 °C. The exothermic effects registered on DTA, in this temperature range are large, suggesting the superposition of two exothermal effects, due to the decomposition of Fe(III) carboxylates and Co(II) carboxylates with formation of the oxides mixture. In the range 300–500 °C, the samples mass remains constant.

Our previous studies [10, 11] on thermal decomposition of Fe(III) and Co(II) homonuclear carboxylates obtained from different diols have evidenced the in situ generation of a reducing atmosphere (CO) during the decomposition. This atmosphere determined the partial reduction of Fe(III) to Fe(II) with re-oxidation to γ-Fe_2O_3 [11] and reduction of Co(II) to Co(0) with re-oxidation to Co_3O_4 and CoO [10]. These redox processes may influence the obtaining of the $Co_xFe_{3-x}O_4$ system.

In order to obtain the oxides mixture, the synthesized precursors were thermally decomposed at 300 °C, for 3 h. The evolution of the oxidic system $Co_xFe_{3-x}O_4$ with the annealing temperature was studied by XRD. In this purpose, the decomposition products were annealed at 400, 700 and 1,000 °C, for 3 h.

Figure 4 presents the XRD patterns for the sample P_5 (with $x = 1$) thermally treated at 300, 400, 700 and 1,000 °C.

The XRD patterns for the decomposition product of the precursor P_5 at 300 °C (Fig. 4 (1)) displays the diffraction peaks characteristic to spinel phases. The large and asymmetric bands suggest the existence of other spinel phases (γ-Fe_2O_3 and Co_3O_4 (JCPDS—International Center for Diffraction Data)) besides cobalt ferrite. By further annealing at 400 °C, no significant changes can be observed regarding the nature and the crystallization degree of the oxides phases (Fig. 4 (2)). The XRD pattern of the sample annealed at 700 °C (Fig. 4 (3)) evidences besides the main crystalline phase $CoFe_2O_4$ (JCPDS—International Center for Diffraction Data), the hexagonal α-Fe_2O_3 as secondary phase. The later crystallises around 500 °C from the spinel phase γ-Fe_2O_3 [11] which forms at low temperatures (300, 400 °C). Pattern (4) of the sample annealed at 1,000 °C evidences the quantitative formation of $CoFe_2O_4$ as sole phase. At this temperature, the unreacted Co_3O_4 turns to CoO which reacts with α-Fe_2O_3 to give cobalt ferrite.

For $x \neq 1$, XRD analysis has evidenced the existence in all samples of other secondary phases besides cobalt ferrite. Figure 5 presents the diffraction patterns of the powders obtained by annealing at 300, 400 and 700 °C of the precursor P_7 (with $x = 1.5$).

Patterns (1) and (2) of the sample P_7 annealed at 300 and 400 °C evidenced the presence of two spinel phases: $CoFe_2O_4$ and Co_3O_4. The annealing at 700 °C (pattern 3) leads to a higher crystallization degree of both major phase ($CoFe_2O_4$) and secondary phase (Co_3O_4). No α-Fe_2O_3 has been evidenced by XRD, resulting that all Fe was present as $CoFe_2O_4$. By annealing at 1,000 °C, Co_3O_4 turns to CoO, whose diffraction peaks superposed with the ones of cobalt ferrite.

In case of the samples synthesized for $x < 1$, the crystalline phases identified within the silica matrix were

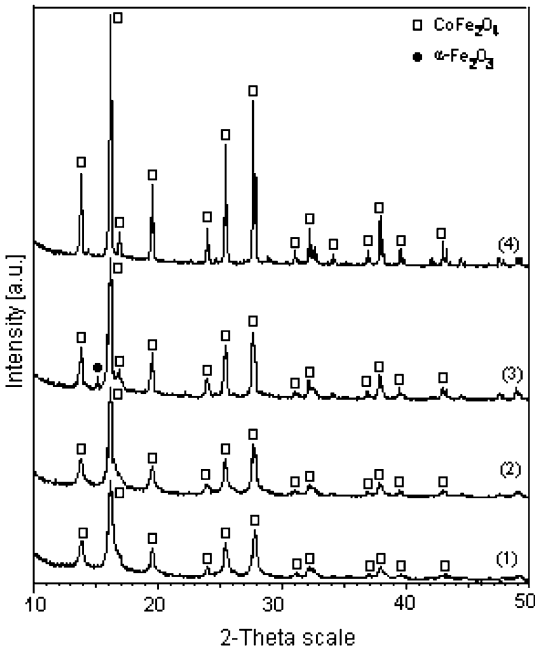

Fig. 4 XRD patterns for the annealing products of the precursor P_5 at 300 °C (1), 400 °C (2), 700 °C (3) and 1,000 °C (4)

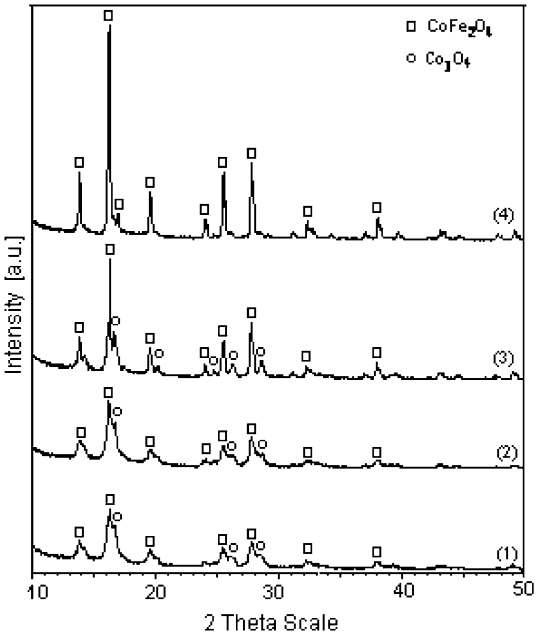

Fig. 5 XRD patterns for the sample P_7 at 300 °C (1), 400 °C (2), 700 °C (3) and 1000 °C (4)

$CoFe_2O_4$ as major phase and γ-Fe_2O_3 or/and α-Fe_2O_3, corresponding to the iron excess.

Figure 6 presents the XRD patterns of the samples obtained by annealing the precursor P_2 ($x = 0.2$) at 300 °C (1), 400 °C (2), 700 °C (3) and 1,000 °C (4). The XRD patterns (1) and (2) of the samples annealed at 300 and 400 °C presented the diffraction peaks characteristic to spinel phases ($CoFe_2O_4$, γ-Fe_2O_3) and traces of α-Fe_2O_3. The sample annealed at 700 °C contains $CoFe_2O_4$ and α-Fe_2O_3 (formed by transformation around 500 °C of γ-Fe_2O_3), both well crystallized. The pattern (4) of the sample annealed at 1,000 °C evidences the same crystalline phases as at 700 °C, but better crystallized.

From the XRD data we have estimated the average diameters of the ferrite crystallites for all temperatures, for the samples P2, P5 and P7, considering the $CoFe_2O_4$ diffraction peaks. The obtained values are presented in Table 2 and indicate that cobalt ferrite is obtained as nanocrystallites.

The magnetic behaviour of all samples approaches to the one of hard magnetic ferrite, with large hysteresis cycles and coercitive field of hundreds of oersted (Figs. 7, 8 and 9). This is due to the very high anisotropy of cobalt ferrite, present in all samples, as shown by XRD (Figs. 4, 5 and 6), which increases the nanoparticles coercivity.

The magnetisation of the samples, measured in 2.15 kOe field, for $x = 1$, 1.5, increases with the temperature of thermal treatment, as it results from the Figs. 7 and 8.

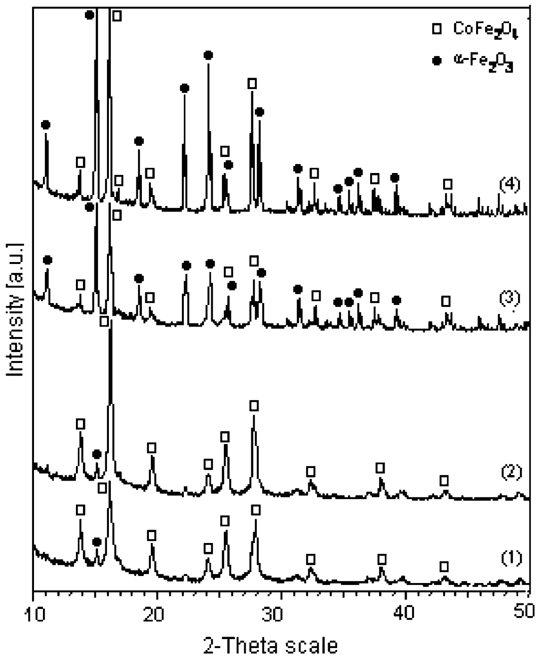

Fig. 6 XRD patterns for the sample P_2 at 300 °C (1), 400 °C (2), 700 °C (3) and 1000 °C (4)

Table 2 Average diameters of the $CoFe_2O_4$ crystallite, obtained with Scherrer equations

Temperature (°C)	Average diameter (nm)		
	P2 ($x = 0.2$)	P5 ($x = 1.0$)	P7 ($x = 1.5$)
400	12	10	11
700	17	15	15
1000	19	17	17

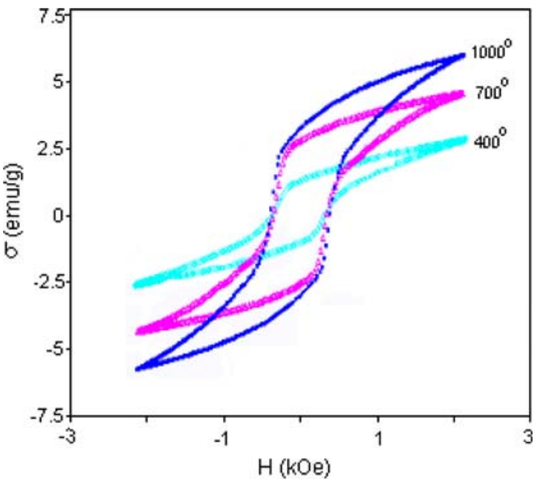

Fig. 7 Magnetisation curves of sample P5 ($x = 1$) annealed at different temperatures

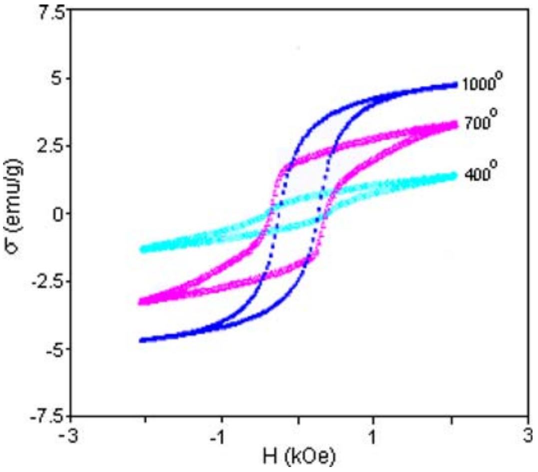

Fig. 8 Magnetisation curves of sample P7 ($x = 1.5$) annealed at different temperatures

These results are in agreement with XRD data (Table 2) which show that the nanocrystallites diameters increase with temperature, leading to the increase of the magnetic moment/nanoparticle.

The samples with $x = 1$ have the most pronounced magnetization, compared with the other samples. For example, the magnetization of the sample P5 annealed at

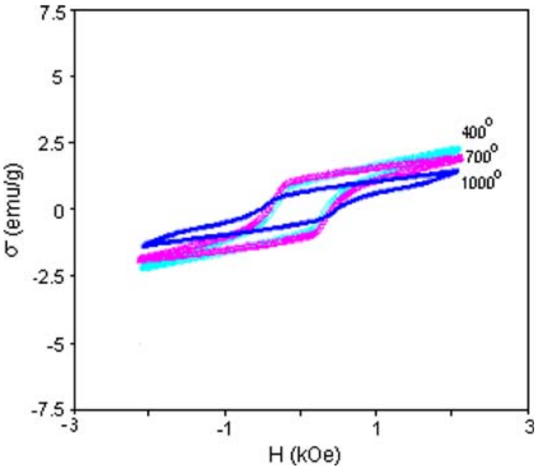

Fig. 9 Magnetisation curves of sample P3 (x = 0.5) annealed at different temperatures

1,000 °C, is of 58.0 emu/g compared with 47.0 emu/g for P7 (x = 1.5) and 13.8 emu/g for P3 (x = 0.5). The lower values of the magnetisation for the other samples are due to the presence of other phases beside cobalt ferrite, as previously showed.

For x = 0.5 the situation is significantly different, the magnetisation decreasing with the temperature despite the increasing of the nanocrystalites dimensions (Table 2).

This behaviour is explained by the presence of the antiferromagnetic α-Fe_2O_3 phase which develops with temperature increase.

Conclusions

The presented study, regarding the preparation of $Co_xFe_{3-x}O_4$ system, has shown that the thermal decomposition of Co(II) carboxylates resulted in the redox reaction between cobalt nitrate and ethylene glycol, allows the preparation of cobalt ferrite $CoFe_2O_4$ as nanoparticles using particular working conditions. For all samples with different x, we obtained at the spinelic phase 300 °C.

For x = 1, we have obtained $CoFe_2O_4$ as major crystalline phase at 700 °C, but it forms quantitatively at 1,000 °C. For $x \neq 1$ ($Co_xFe_{3-x}O_4$), we have obtained besides cobalt ferrite ($CoFe_2O_4$) the secondary phases: Fe_2O_3 (for $x < 1$) and Co_3O_4 (for $x > 1$).

The magnetic properties of the nanoparticles system can be controlled both by x and the thermal treatment temperature. All samples have a hard magnetic behaviour due to the high anisotropy of cobalt ferrite.

Acknowledgements This work was supported by the National Project No. 71-026 NANOPART and financed by CNMP-ANCS through Romanian Ministry of Education and Research.

References

1. Kubota M, Kanazawa Y, Nasu K, Moritake K, Kawaji H, Atake T, Ichiyanagi Y. Effect of heat treatment on magnetic $MgFe_2O_4$ nanoparticles. J Therm Anal Calorim. 2008;98:461–63.
2. Mendelovici E, Villalba R, Sagarzazu A. Distinctive cobalt ferrites prepared by the thermal-transformation alkoxide route. Thermochim Acta. 1998;318:51–6.
3. Franco Jr A, Lima ECO, Novak MA, Wells PR. Synthesis of nanoparticles of $Co_xFe_{(3-x)}O_4$ by combustion reaction method. J Magn Magn Mater. 2007;308:198–202.
4. Liu C, Rondione AJ, Zhang ZJ. Synthesis of magnetic spinel ferrite $CoFe_2O_4$ nanoparticles from ferric salt and characterization of the size-dependent superparamagnetic properties. Pure Appl Chem. 2000;72:37–45.
5. Franco Jr A, Zapf V. Temperature dependence of magnetic anisotropy in nanoparticles of $Co_xFe_{(3-x)}O_4$. J Magn Magn Matter. 2008;320:709–13.
6. Li X, Kutal C. Synthesis and characterization of superparamagnetic $Co_xFe_{3-x}O_4$ nanoparticles. J Alloys Comp. 2003;349: 264–8.
7. Cote LJ, Teja AS, Wilkinson AP, Zhang ZJ. Continuous hydrothermal synthesis of $CoFe_2O_4$ nanoparticles. Fluid Phase Equilibria. 2003;210:307–17.
8. Chirtop E, Mirtov I, Ion RM, Iliescu M. A low temperature path to the preparation of $CoFe_2O_4$ ferrite. J Optoel Adv Mater. 2000;2(4):379–84.
9. Horng L, Chern G, Chen MC, Kang PC, Lee DS. Magnetic anisotropic properties in Fe_3O_4 and $CoFe_2O_4$ ferrite epitaxy thin films. J Magn Magn Mater. 2004;270:389–96.
10. Dippong T, Stoia M, Stefanescu M. Study on the obtaining of Co_xO_y starting from $Co(NO_3)_2\cdot6H_2O$ and ethylene glycol. Proceeding of XIVth, symposium on analytical and environmental problems, 24 September 2007, Szegen, Hungary, p. 134–8.
11. Stefanescu M, Stefanescu O, Stoia M, Lazau C. Thermal decomposition of some metal-organic precursors. Fe_2O_3 nanoparticles. J Therm Anal Cal. 2007;88:27–32.
12. Stefanescu M, Dippong T, Stoia M, Stefanescu O. Study on the obtaining of cobalt oxides by thermal decomposition of some complex combinations, undispersed and dispersed in SiO_2 matrix. J Therm Anal Calorim. 2008;94:389–93.
13. Prasad R, Sulaxna, Kumar A. Kinetics of thermal decomposition of iron(III) dicarboxylate complexes. J Therm Anal Calorim. 2005;81:441–50.